Jurnal Teknologi

Full Paper

INFLUENCE OF COIR FIBRES AND EXTRUSION PROCESS PARAMETERS ON RECYCLED PLA FILAMENT STRENGTH USING TAGUCHI-GRA METHOD

Amirah R. Suryanto[a], Herianto[a], Ihwan Ghazali[b], Achmad, P. Rifai[a], Wangi P. Sari[a*]

[a]Department of Mechanical and Industrial Engineering, Faculty of Engineering Universitas Gadjah Mada, Jalan Grafika No. 2 Yogyakarta 55281, Indonesia

[b]Faculty of Industrial and Manufacturing Technology and Engineering, Universiti Teknikal Malaysia, Melaka, Hang Tuah Jaya, Durian Tunggal 76100, Melaka, Malaysia

Article history
Received
3 September 2024
Received in revised form
9 July 2025
Accepted
9 July 2025
Published Online
16 June 2026

*Corresponding author
wangipandansari@ugm.ac.id

Graphical abstract

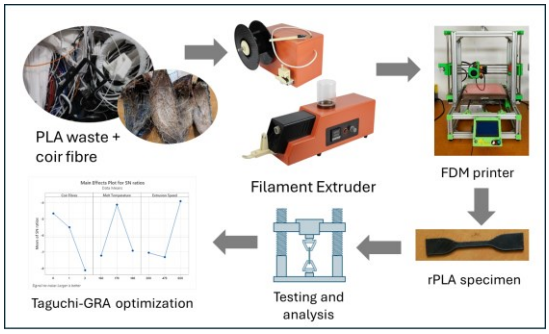

Abstract

The widespread adoption of 3D printing using Fused Deposition Modelling (FDM) has led to a significant accumulation of Polylactic Acid (PLA) waste. This study aimed to address this environmental concern by recycling PLA waste into recycled PLA (rPLA) filaments and exploring the potential enhancement of their mechanical properties through the addition of coir fibre reinforcement. Design of Experiments (DoE) approach using Taguchi orthogonal arrays and Grey relational analysis was employed to assess impact of coir fibre addition and extrusion process parameters on the mechanical properties of rPLA filaments. The analysis revealed that coir fibre reinforcement did not significantly improve mechanical properties and the optimal extrusion conditions for maximizing ultimate tensile strength (UTS) and elongation at break were identified at a melt temperature of 170°C, and an extrusion speed of 650 mm/min. Under these conditions, rPLA filaments achieved a UTS of 17.02 MPa and an average elongation at break of 1.09%. The study successfully demonstrated the feasibility of recycling PLA waste into rPLA to contribute to a more sustainable 3D printing industry.

Keywords: Fused deposition modelling, Taguchi, Grey Relationship Analysis, recycled PLA, Material extrusion

1.0 INTRODUCTION

Additive manufacturing (AM), also known as 3D printing, is an advanced manufacturing technique that constructs 3D objects through a layer-by-layer addition process. This method offers several advantages over conventional manufacturing techniques, which typically involve subtracting material from a larger workpiece. AM enables the production of complex geometries that would be

otherwise difficult or impossible to achieve using traditional methods. It effectively addresses challenges such as low production volumes, high design complexity, and frequent design changes [1]. Based on statistical data in 2018, AM technology developed by 18% and is estimated to increase to 26% in 2026 [2]. It has been used in a wide range of industries such as aerospace [3, 4, 5], healthcare [6, 7], fashion [8, 9], and consumer goods [10, 11]. Several common techniques of AM include Stereolithography (SLA), Selective Laser Sintering (SLS), and Fused Deposition Modelling (FDM).

FDM is the most commercially available printing technique, projected to grow at a CAGR of 32.11% from 2023 to 2028 according to Global Market Estimates [12]. This growth is attributed to the technology's low costs, ease of printing, material flexibility, availability, and application simplicity. Common materials used in FDM include ABS (acrylonitrile butadiene styrene), PLA (polylactic acid), nylon/polyamide, ASA (acrylonitrile styrene acrylate), PET (polyethylene terephthalate), PETG (polyethylene terephthalate glycol-modified), and PC (polycarbonate), with ABS, PLA, and nylon being the most popular due to their low melting temperatures [13]. PLA is particularly favoured in FDM due to its low glass transition temperature (Tg = 60-65°C) and melting temperature (Tm = 173-178°C), which simplify the printing process as they do not require a heated print bed [14]. However, the widespread use of PLA also leads to environmental and efficiency challenges, as the material contributes to significant waste from supports, experimental artifacts, and failed prints. Despite these issues, the demand for PLA filament continues to rise, with an annual growth rate of up to 20% [15]. Fortunately, the waste generated from 3D printing with PLA can be reprocessed into new filament, offering a potential solution to mitigate environmental impact.

PLA material can undergo structural changes when liquefied and cooled during FDM printing, which can affect its characteristics [16]. This is due to thermal degradation, which can reduce molecular weight and crystallinity. Consequently, objects printed using recycled PLA filament (rPLA) may exhibit decreased tensile strength and altered morphology compared to those printed using virgin PLA. Numerous studies have aimed to enhance the performance of PLA filaments by creating composite materials. For instance, incorporating additives such as carbon fibre [17], [18], [19] and graphene [20], [21], [22] into PLA has been shown to improve its mechanical properties. Given the success of these approaches with virgin PLA, it is reasonable to expect that integrating similar additives into rPLA could also enhance the performance of rPLA filaments. However, these additives are often expensive and difficult to use for practical purposes [23].

Biopolymers reinforced with natural fibres have a positive environmental impact due to their sustainable composition. The unique cell structure of natural fibres, composed of cellulose microfibrils embedded in a lignin and hemicellulose matrix [24], provides desirable properties for reinforcement. One readily available natural fibre, particularly in Indonesia, is coir fibre (CF). Coir fibre has a low cellulose (40–43%) and hemicellulose (0.15–0.25%) content and a high lignin content (41–45%) [25]. Coir fibre was selected for this study due to its high availability in Indonesia, cost-effectiveness, and environmental sustainability. It is a widely available agricultural byproduct rich in lignin, making it relatively stiff and durable among natural fibres. Its use supports the valorization of local biomass resources and contributes to developing more sustainable 3D printing materials. Coir fibre has been studied extensively as a reinforcing material for various polymers and plastics, including TPS, polypropylene, and PLA [26], [27]. Previous study has shown that TPS/PLA/CF composites, processed using extrusion and injection moulding methods, exhibit a continuous structure with increased stiffness and hardness [28]. Another study investigated the effect of particle size and raster angle on the mechanical properties of the PLA/CF composite [29]. For instance, several studies have emphasized the importance of chemical treatments such as alkalization and silanization in enhancing the compatibility between natural fibres and PLA matrices. PLA composites reinforced with treated flax fibres have been shown to achieve a 120% increase in impact strength and a 31.2% increase in tensile elongation compared to neat PLA [30]. Another study reported that the tensile strength of alkali-treated flax fibre composites increased significantly, reaching up to 50 MPa [31].

Despite the considerable research on CF as a reinforcement in various polymer matrices, there has been a lack of studies specifically incorporating CF into rPLA. Moreover, filament production for FDM, particularly involving composite materials, faces challenges related to dimensional accuracy, consistent melting, and extrusion stability [32]. Therefore, this study aims to fill in the gap in the literature by assessing the influence of CF and extrusion process parameters on the mechanical strength of rPLA.

2.0 METHODOLOGY

2.1 Specimen Fabrication

Recycled PLA pellets were created from PLA 3D printing waste that has been shredded first with a length of 3-5 mm (Figure 1). Coir fibres, extracted from coconut husk sourced from Temon, Kulon Progo, were cut with around 4 mm length (60 grams) before added to 1 liter of a mixture containing 160 ml of hydrogen peroxide (H2O2) and 0.5 grams of sodium peroxide and stirred for 1 hour. Afterward, the coir fibres were rinsed using distilled water and dried using

an oven at 100°C for 12 hours. The preparations flow of coir fibre is shown in Figure 2.

According to the preliminary experiments, rPLA was very brittle hence it was subsequently mixed with virgin PLA pellets measuring 2-3 mm (NV = EX2001; purchased from Indofilam) at 50%-50% ratio. Before use, rPLA pellets and virgin PLA pellets were dried using an oven at 100°C for 2 hours to reduce the water content. The mixture of rPLA, virgin PLA, and coir fibres was melted and extruded using a Wellzoom Filament Extruder. This device is a compact single-screw extruder with a screw diameter of 16 mm and a length-to-diameter (L/D) ratio of 15:1, equipped with a PID-controlled heating system and adjustable speed via a stepper motor. It supports various thermoplastics, including PLA, ABS, and wood-plastic composites, and can operate at temperatures up to 300°C. The extruder uses a 1.75 mm nozzle, with an extrusion accuracy maintained within ±0.05 mm.

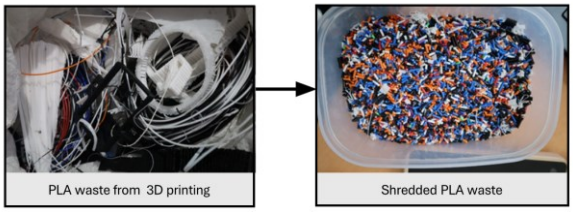

Figure 1 PLA Waste Preparations

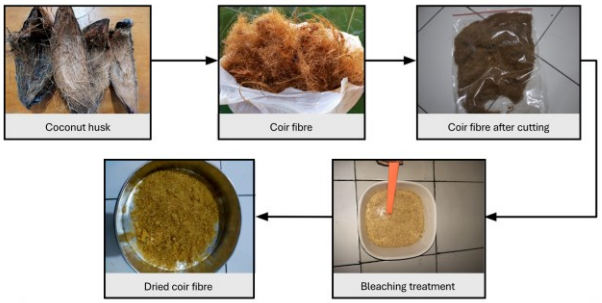

Figure 2 Coir fibres preparations

2.2 Design of Experiments (DOE)

This study evaluates three factors, i.e., ratio of coir fibre content, melting temperature, and extrusion speed. Each factor was tested at three levels, as shown in Table 1, to determine their impact on the filament strength.

Table 1 Influencing factors and level for each factor

Coir Fibres (wt%)	Melt Temperature (℃)	Extrusion Speed (mm/min)
0	160	300
1	170	475
3	180	650

Taguchi method was employed using an orthogonal array (OA) to optimise the extrusion parameters for recycled PLA filament. Instead of testing every possible combination of levels across all factors, this method is designed to cover the parameter space efficiently by capturing the main effects and sufficient interaction effects with fewer experiments. The size of an OA depends on the number of factors and levels and degrees of freedom of the parameters selected. This study used L9 (3^3) OA as shown in Table 2. Each run was duplicated three times, creating 27 total specimens.

2.3 Experimental Setup

To assess the mechanical properties of the extruded filament, tensile tests were conducted using the CRN-50 Ultimate Tensile Machine (Carson Technology Testing Equipment Co. Ltd.). The filament samples prepared for testing had a diameter of 0.75 mm and a length of 150 mm. The tensile speed used in the experiment was 0.5 mm/min. It was selected to ensure precise load application on the small-diameter specimens and to minimize strain rate effects.

Table 2 L9 orthogonal array

Run	Code	Coir Fibres (wt%)	Melt Temp(℃)	Extrusion Speed (mm/min)
1	0-160-300	0	160	300
2	0-170-475	0	170	475
3	0-180-650	0	180	650
4	1-160-475	1	160	475
5	1-170-650	1	170	650
6	1-180-300	1	180	300
7	3-160-650	3	160	650
8	3-170-300	3	170	300
9	3-180-475	3	180	475

For validating the experimental outcomes, the optimized combination of coir fibre content, melting temperature, and extrusion speed was selected for extrusion. The filament was subsequently printed using an FDM printer following the ASTM D638 type IV standard (Figure 3). The dimensions of the specimen were 115×19×3.4 mm. While ASTM D638 recommends a 5 mm/min crosshead speed for Type IV specimens, a reduced speed of 2 mm/min was used in this study. This adjustment was based on preliminary trials that revealed the brittle nature of the recycled PLA composites caused premature failure when tested at higher speeds. The lower speed allowed for smoother load application and better consistency in capturing tensile properties.

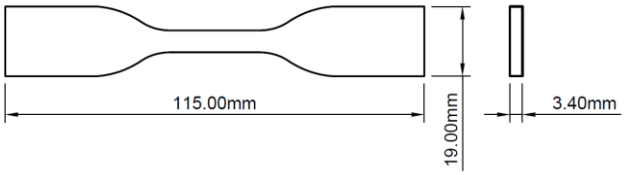

Figure 3 Specimen dimension according to ASTM D638 type IV standard

Printing parameters used were as follows: nozzle diameter of 0.4 mm, layer thickness of 0.15 mm, hot-end temperature of 220°C, bed temperature of 60°C, infill percentage of 100%, infill pattern of lines, and print speed of 70 mm/s. The specimens' morphology was captured using a digital microscope Dino-Lite/1,3MP series AF4915 analysed using ImageJ software. The cross-sectional images of fractured specimens were processed by converting the images to grayscale. Subsequently, the images were binarized using an optimized threshold. The total pore area was determined using the "Analyze Particles" tool, and porosity was calculated as the percentage of pore area relative to the total cross-sectional area.

Tensile properties were selected as the focus of this study due to their sensitivity to material defects and their relevance in evaluating the structural integrity of FDM-printed parts. Since rPLA and fibre-reinforced composites are prone to issues such as poor interfacial adhesion and increased porosity, tensile tests provide a robust basis for assessing performance under load.

2.4 Analysis using Taguchi

Using the Taguchi method, experimental data were transformed into signal-to-noise (S/N) ratios. S/N ratios quantify the influence of factors on a response by maximizing the "signal" (desired outcome) and minimizing the "noise" (undesirable variations). The S/N ratio is used to see which factors have the most influence on the experimental results. Three types of S/N ratio characteristics include smaller is better, nominal is the best, and larger is better.

For this experiment, where the goal was to maximize the tensile properties of a material, a 'larger is better' S/N ratio was employed. This means that factors leading to higher tensile values would result in larger S/N ratios. The formula to calculate this approach is shown in Eq. (1), where η equals to S/N ratio, n represents the number of repetitions, and Y_i represents the i^{th} individual experiment result.

$$\eta = -10 \log\left[\frac{1}{n}\sum_{i=1}^{n}\frac{1}{Y_i^2}\right] \quad (1)$$

The Taguchi method was chosen for this study due to its simplicity, efficiency, and suitability for early-stage optimization. Compared to other factorial or response surface designs such as Box-Behnken Design (BBD) or Central Composite Design (CCD), the Taguchi method enables significant reduction in the number of experimental runs while still identifying the most influential factors affecting the responses. This is particularly important given the resource constraints associated with processing recycled PLA and natural fibre reinforcements. Moreover, to address the multi-response nature of the study, the Taguchi method was integrated with Grey Relational Analysis (GRA). This combined approach allows for effective simultaneous optimization of multiple performance characteristics without the need for complex response surface modeling.

2.5 Grey Relational Analysis

Grey Relational Analysis (GRA) is a statistical method that combines multiple performance characteristics into a single value, allowing for the optimisation of control parameters with multi-responses. This approach utilizes the Grey Relational Grade (GRG) to optimize parameters based on their effects on the responses [30]. First, each performance characteristic's data must be pre-processed to enable comparison across various scales and units. This pre-processing involves normalizing the data so that each factor's impact is equally considered, regardless of its original magnitude or unit. As the response for tensile data is expected to be larger, *"larger is better"* is chosen. The equation is shown in Eq (2), where x_{ij}^* is the normalised value, x_{ij} is the original S/N ratio value of the i-th experiment for the j-th performance characteristics, min (x_{ij}) and max (x_{ij}) are the minimum and maximum values of the j-th performance characteristic across all experiments, respectively.

$$x_{ij}^* = \frac{x_{ij} - \min(x_j)}{\max(x_{ij}) - \min(x_{ij})} \quad (2)$$

Following normalization, the next step involves calculating the Grey Relational Coefficient (GRC) for each response. This coefficient measures the closeness of the given alternative to the ideal solution. The GRC is computed using a formula that considers both the deviation of each alternative from the ideal, and a distinguishing coefficient which helps modulate the influence of the deviation on the final result. The deviation sequence and the GRC formula are shown in Eq (3) and (4) respectively, where Δ_{ij} represents the deviation, x_0^* is ideal (best) normalized value for the performance characteristic, typically taken as 1 for "larger is better", x_{ij}^* is the normalized value of the i -th experiment for the j-th performance characteristic, ξ_{ij} is the GRC value of the i -th experiment for the j-th performance characteristic; Δ_{min} and Δ_{min} are the minimum and maximum deviations across all experiments for all characteristics, and ζ is the distinguishing coefficient

(also known as the resolution coefficient), which is a user-defined parameter typically set between 0 and 1(in this study it is set at 0.5).

$$\Delta_{ij} = \left| x_0^* - x_{ij}^* \right| \quad (3)$$

$$\xi_{ij} = \frac{\Delta_{min} + \Delta\zeta_{max}}{\Delta_{0i}(k) + \Delta\zeta_{max}} \quad (4)$$

Once all GRCs are calculated, they are aggregated into the Grey Relational Grade (GRG). This grade is a weighted sum of the GRCs, where weights reflect the relative importance of each response in the multi-response scenario. A higher GRG indicates a better overall performance of the parameter settings under consideration. GRG formula is shown in Eq (5), where y_i represents (GRG) for the i -th experiment; n is the total number of performance characteristics or criteria evaluated in the experiment, ξ_{ij} is the GRC value of the i -th experiment for the j-th performance characteristic.

$$y_i = \frac{1}{n}\sum_{j=1}^{n} \xi_{ij} \quad (5)$$

While Young's modulus is an important mechanical property representing material stiffness, it was not included in this study's optimization scope. The focus was directed toward UTS and elongation at break, as these properties are more sensitive to recycled material degradation and more relevant for FDM applications where tensile failure is often critical. Moreover, limiting the analysis to two outputs enabled a clearer implementation of the Taguchi-GRA method in this preliminary investigation.

3.0 RESULTS AND DISCUSSION

3.1 Ultimate Tensile Strength

Figure 4 shows the average and standard deviation of the ultimate tensile strength (UTS) of extruded and commercial filaments. Extruded filaments generally display a lower average UTS compared to commercial filaments, as indicated in the graph. Extruded filaments with the highest UTS results are filaments with variations of 1% coir fibres, melt temperature 170℃, and extrusion speed 650 mm/min. This may be attributed to more effective dispersion of coir fibres at this setting, which can enhance stress transfer between the matrix and fibres. In contrast, during extrusion trials, it was qualitatively observed that at 160°C, the rPLA-coir mixture became more viscous and prone to premature solidification inside the barrel, leading to flow instability and partial clogging. At 180°C, however, the melt became excessively fluid, which likely reduced shear forces and hindered fibre dispersion, resulting in agglomeration. This behavior aligns with findings from Abeykoon *et al.*, where underheating leads to inadequate melt fluidity and poor fibre mixing, while overheating causes thermal degradation and disrupts fibre distribution uniformity, both of which compromise mechanical performance [34], [35]. Additionally, the extrusion speed significantly influences the UTS; higher speeds tend to increase the UTS. However, increasing the coir fibre content leads to fibre accumulation at several points, consequently lowering the UTS of the resulting filament.

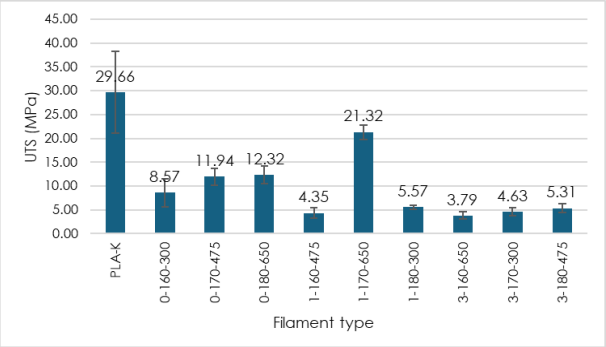

Figure 4 UTS of the extruded filaments compared with commercial PLA

S/N ratio for the UTS is shown in Figure 5. The highest S/N ratio is obtained when no coir fibres added. As the coir fibre content increases, there is a noticeable decline in the S/N ratio. This result is different from the previous where the highest UTS observed from filament with 1% coir fibre. This is probably because filaments without coir fibre exhibits less variability and those with coir fibre show higher variability due to uneven distribution of fibres. Furthermore, the reduction in UTS with increasing coir fibre content may also stem from the intrinsic incompatibility between the hydrophilic nature of untreated coir fibres and the hydrophobic PLA matrix. This mismatch can result in poor interfacial adhesion and inadequate stress transfer, promoting interfacial debonding and fibre pull-out during tensile loading [36], [37] Such weak bonding acts as stress concentrators, thereby reducing the composite's load-bearing capability. For the melt temperature, the S/N ratio peaks at 170°C. Lower and higher temperature resulted in lower S/N ratio, consistent with the findings from Figure 4. Extrusion speed also shows similar results where the highest S/N ratio achieved from the higher extrusion speed.

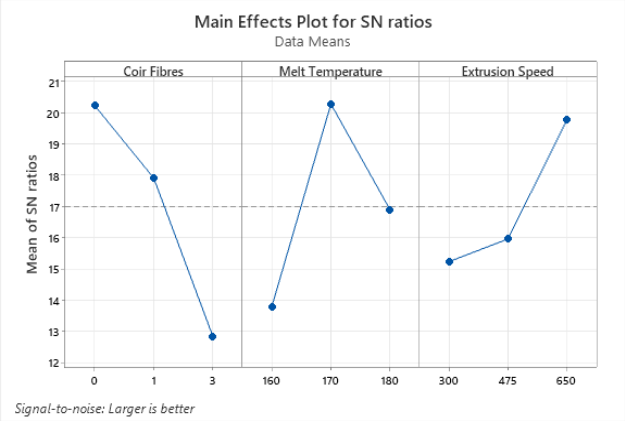

Figure 5 Main plot graph for ultimate tensile strength

3.2 Elongation at Break

Figure 6 displays the average and standard deviation of the elongation at break of commercial filaments and extruded filaments. Based on the data obtained, all extruded filaments have a lower elongation at break compared to commercial filaments. This shows that commercial PLA have better ductility compared to recycled filaments. This is expected as extruded filaments have experienced degradation when reheated and contain more porosity than commercial filaments. As measured from cross-sectional images using ImageJ, the porosity of rPLA specimens averaged 28.2%, compared to just 5.2% in commercial PLA. Higher porosity increases the number of voids and discontinuities within the material, which act as stress concentration points and inhibit plastic deformation. This leads to earlier crack initiation and brittle failure, thus reducing the material's ductility and elongation at break.

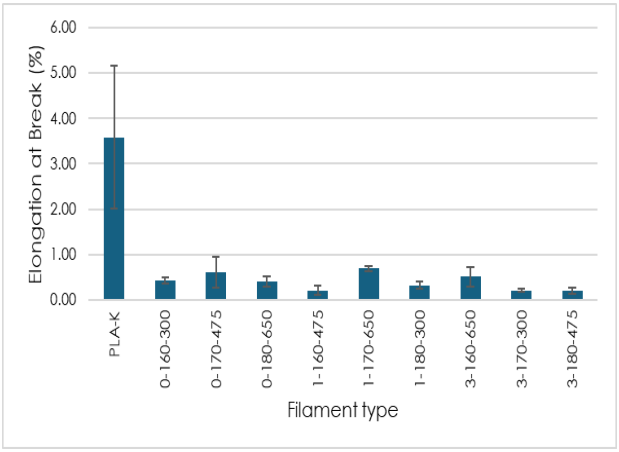

Figure 6 Elongation at break of the extruded filaments compared with commercial PLA

Consistent with the UTS findings, the highest S/N ratio is observed from extruded filaments with no coir fibre (Figure 7). The elongation at break decreased with higher fibre content, which can be attributed to weak fibre–matrix interactions that limit the material's ability to undergo plastic deformation before fracture. Several studies have similarly reported that increasing fibre content in composite filaments generally leads to a decrease in elongation at break due to poor interfacial bonding between the fibre and matrix [36], [37], [38]. This incompatibility is especially common when untreated natural fibres are blended with hydrophobic polymers like PLA, resulting in reduced mechanical performance due to fibre pull-out and interfacial failure [36], [37].

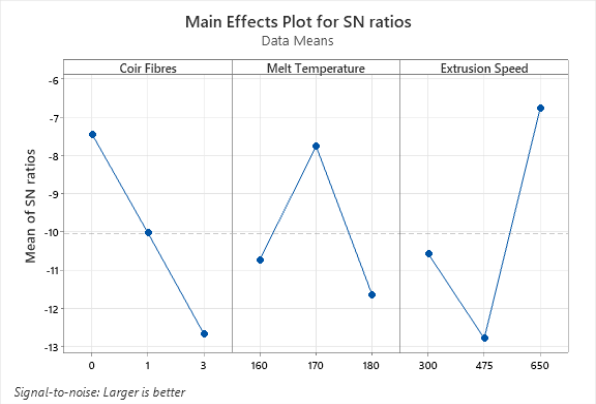

Figure 7 Main plot graphs for elongation at break of the extruded filaments

Similarly, the highest S/N ratio is observed from filaments extruded at 170°C and with extrusion speed of 650 mm/min. This temperature likely facilitated sufficient chain mobility and interlayer diffusion, which are critical for ductile behavior during tensile deformation [39], [40]. In glassy polymers like PLA, tensile stress lowers potential energy barriers, enhancing molecular mobility and narrowing relaxation time distributions—ultimately improving local homogeneity and cohesive strength [41]. In addition, diffusion mechanisms such as chain hopping enable polymer chains to disengage and redistribute across interfacial boundaries, further promoting interlayer bonding [42]. These mechanisms contribute to improved resistance to fracture by enhancing structural continuity between extruded layers. At lower temperatures, limited polymer flow may result in weak layer adhesion and elevated internal stresses, thereby restricting elongation [43]. Conversely, excessive temperatures can trigger thermal degradation and reduce molecular weight, compromising the material's ability to undergo plastic deformation [35]. In terms of extrusion speed, higher speeds can lead to smoother filament surfaces and reduce cooling-induced irregularities, thereby minimizing early crack initiation sites and supporting better ductile performance [44].

3.3 Multi-response Optimisation using GRA

S/N ratio for multi-response optimisation was obtained after calculating the GRG (Table 3). The effect of each parameter on tensile properties can be seen through the main plot graph (Figure 8) to determine the optimal parameters.

Table 3 S/N ratio for multi-response optimisation using GRG

No	GRG	S/N Ratio
1	0.54	-5.39
2	0.64	-3.86
3	0.58	-4.76
4	0.34	-9.33
5	1.00	0.00
6	0.44	-7.23
7	0.45	-7.00
8	0.37	-8.59
9	0.36	-8.82

The main effect graph shown in Figure 8 shows that the optimal parameters used are coir fibres 0 wt.%, melt temperature 170℃, and extrusion speed 650 mm/min. Increasing the coir fibre content causes a decrease in the tensile properties of the filament. It can be observed that increasing the content of coir fibres reduces the tensile properties of the filament, primarily due to fibre agglomeration and uneven distribution of fibre, which cause localised stress concentrations and premature failure. Several studies have shown that untreated natural fibres like coir tend to form clusters within polymer matrices and suffer from poor interfacial bonding with PLA due to surface incompatibility [36], [37].

The melt temperature presents an optimal value at 170°C, declining at higher and lower temperatures. At temperatures above 170°C, rPLA becomes too fluid, hindering the uniform extrusion of coir fibres and potentially causing blockages in the extrusion process. At a lower temperature of 160°C, rPLA mixed with coir fibres tends to harden more rapidly within the extrusion machine. This premature hardening can create difficulties during the extrusion process, as the increased viscosity at this lower temperature makes it harder for the filament to flow smoothly through the extruder. This observation is supported by Abeykoon *et al*. [34], [35], who demonstrated that both underheating and overheating in polymer extrusion compromise fibre distribution and melt homogeneity.

On the other hand, the extrusion speed parameter shows an increase in tensile properties at the highest speed. At lower speeds, the filament tends to develop a wavy surface which can negatively affect its mechanical strength and uniformity. Adjusting the extrusion rate has been shown to significantly affect surface quality. Wang *et al*. [45] demonstrated that correcting the extrusion flow rate can reduce surface defects and improve wall thickness accuracy in thin-walled models. Additionally, in high-speed extrusion scenarios, surface finish may deteriorate due to heat buildup and flow instability; however, optimized material formulations or controlled speed adjustments can mitigate these effects [46]. While some studies suggest speed may have a limited impact within certain ranges [47], ensuring consistent flow and cooling conditions remains key to achieving smoother filament surfaces and improved mechanical performance.

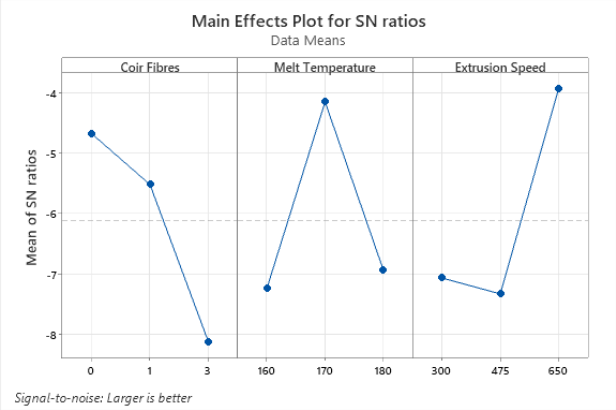

Figure 8 Main plot graphs for multi-responses optimization of the extruded filaments

Figure 9 presents two 3D printed specimens: one fabricated from commercial PLA and the other from rPLA composite. A noticeable difference between the two is that the rPLA specimen has a rougher and more uneven surface compared to the smooth and uniform surface of the commercial PLA specimen. The variance in surface quality can be attributed to several factors associated with the materials used and the extrusion process. Firstly, rPLA often contains impurities due to the recycling process, which can affect the consistency of its melting and extrusion properties and lead to a rougher surface finish. In contrast, commercial PLA is manufactured with precise control over its properties to ensure it melts and extrudes smoothly, thus resulted in a finer surface finish.

Figure 9 ASTM D638 Type IV commercial PLA (left) and rPLA specimens (right)

The parameter combination of 0 wt% coir fiber, 170°C melt temperature, and 650 mm/min extrusion speed (coded as 0-170-650) was identified as the optimal setting based on the highest Grey Relational Grade (GRG) from the multi-response optimization. This setting was selected for the confirmation experiment and used as the basis for comparison with commercial PLA in order to evaluate the mechanical performance of optimized recycled PLA filaments under standardized testing. Tensile testing was carried out with the ASTM D638 type IV standard design. The tensile test data in Table 4 show that both the ultimate tensile strength and elongation at break of the commercial white PLA specimen have higher values than the rPLA specimen. To ensure a fair comparison, the commercial PLA specimens were printed using the same printing parameters as the optimized rPLA filament under the 0-170-650 condition.

The tensile testing conducted in accordance with ASTM D638 Type IV standard reveals differences in the mechanical properties of commercial white PLA and rPLA specimens, as detailed in Table 4.

Table 4 Specimens' UTS and Elongation at breaks compared to prediction

Type		Commercial PLA	rPLA (0-170-650)
Ultimate Tensile Strength (MPa)	1	38.28	18.08
	2	38.04	16.63
	3	41.41	16.34
Means		39.24	17.02
Predicted UTS		23.56	18.76
Elongation at Break (%)	1	3.37	1.09
	2	2.58	0.93
	3	2.06	1.25
Means		2.67	1.09
Predicted Elongation		2.57	0.72

The results show that commercial PLA specimens consistently exhibit superior performance in both UTS and elongation at break compared to rPLA specimens. UTS of commercial PLA filaments is averaged at 39.24 MPa, significantly exceeding the predicted UTS of 23.56 MPa. On the other hand, extruded rPLA specimens demonstrate UTS value at 17.02 average, closely aligning with the predicted value of 18.76 MPa. Commercial PLA shows elongation at break with a mean value of 2.67%, which is closely accurate with the prediction at 2.57%. However, rPLA specimens exhibit much lower elongation rates with an average of 1.09%. Despite being lower, these figures slightly exceed the predicted elongation of 0.72%. It is worth noting that although the optimal parameter combination (0 wt% coir fibre, 170°C melt temperature, 650 mm/min extrusion speed) matches the settings used in Run 5 of the Taguchi L9 orthogonal array, a direct comparison between these two results is not appropriate. This is because the DOE experiments were conducted on extruded filament samples, whereas the confirmation test involved 3D printed ASTM D638 Type IV specimens. Differences in geometry, layer deposition, and stress distribution during printing affect the mechanical performance, making the results inherently different. However, the consistency in identifying the same parameter combination as optimal in both experimental stages emphasizes the reliability of the optimization

Specimens' morphology can be seen in Figure 10. As noted in Section 3.2, ImageJ analysis of cross-sectional micrographs revealed that extruded filament specimens exhibited an average porosity of 28.2%, significantly higher than the 5.2% measured in commercial PLA specimens. The elevated porosity in the rPLA specimens can be attributed to several factors. First, the recycling process involves repeated thermal exposure, which promotes chain scission and reduces melt viscosity, increasing the likelihood of void formation. Second, residual moisture—even after drying—may lead to hydrolytic degradation and vapor formation during extrusion. Third, the incorporation of untreated coir fibres can further increase porosity due to poor dispersion and weak interfacial adhesion, which prevent the polymer matrix from fully encapsulating the fibres and introduce internal voids.

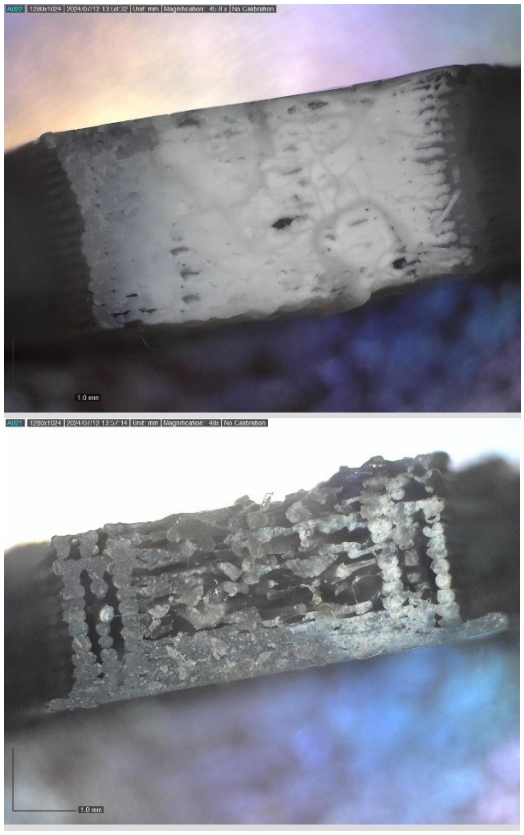

Figure 10 Fracture Cross-section of Commercial Filament Specimen (left) and Extruded Filament (right)

This higher porosity in the rPLA specimens contributes directly to their decreased tensile properties when compared to the commercial filaments. The reduced material density from higher porosity leads to poor compaction and less adhesive interactions between filament layers, which compromises the structural integrity and mechanical strength of the rPLA. This is consistent with findings from Klosterman *et al*. [48], who reported that higher porosity leads to easier horizontal propagation of cracks between layers, reducing strength and increasing the likelihood of failure. The observed fracture surfaces corroborate these findings: the commercial filament fractures were cleaner and smoother, indicative of a more brittle fracture that typically occurs in denser, less porous materials. Conversely, the rPLA specimens displayed rougher fracture surfaces, aligning with findings from [49], which noted similar characteristics comparing virgin PLA to rPLA. The rPLA fractures were more ductile with little plastic deformation, suggesting that the material absorbed more energy before fracturing, a typical characteristic of materials with higher porosity and rougher texture.

Overall, the inferior performance of rPLA compared to commercial virgin PLA in terms of strength and elasticity can be attributed to the degradation of polymer chains during the recycling process, which results in shorter chains and less uniform material properties. Thermal degradation typically results in a decrease in molecular weight, which is closely associated with a decline in mechanical properties such as tensile strength and impact resistance [50], [51], [52]. Additionally, impurities and variability in the recycling process can further compromise these properties. While rPLA offers a sustainable alternative by utilizing recycled materials, its application in high-strength or high-flexibility scenarios is compromised.

4.0 CONCLUSION

In this study, rPLA, derived from 3D printing waste, has been reprocessed to create FDM filament. The study assessed the effects of incorporating coir fibers as a reinforcing material and varying extrusion process parameters (melting temperature and extrusion speed) on the Ultimate Tensile Strength (UTS) and elongation at break. The experimental results were statistically analyzed using the S/N ratio and Grey Relational Analysis methods. The results show that the optimal combination for tensile properties includes 0% coir fibers, a melt temperature of 170℃, and an extrusion speed of 650 mm/min. The UTS and elongation at break of rPLA were found at lower values compared to commercial PLA filaments. This underscores the need for further refinement in processing techniques and possibly material formulations to enhance the properties of recycled filaments. Future research should focus on optimizing the recycling processes and exploring additives or modifiers that could reinforce the mechanical properties of rPLA without compromising its recyclability and environmental benefits.

Acknowledgement

The authors would like to thank the Department of Mechanical and Industrial Engineering, Faculty of Engineering, Universitas Gadjah Mada, Indonesia, for providing the facilities and resources necessary to conduct this research

Conflicts of Interest

The authors declare that there is no conflict of interest regarding the publication of this paper.

References

[1] Abdulhameed, O., A. Al-Ahmari, W. Ameen, and S. H. Mian. 2019. Additive Manufacturing: Challenges, Trends, and Applications. *Advances in Mechanical Engineering*. 11(2): 1687814018822880.

[2] Syaifuddin, M., H. Suryanto, and S. Suprayitno. 2021. The Effect of Multi-Extrusion Process of Polylactic Acid on Tensile Strength and Fracture Morphology of Filament Product. *Journal of Mechanical Engineering Science and Technology*. 5(1): 62–72.

[3] Schiller, G. J. 2015. Additive Manufacturing for Aerospace. In *2015 IEEE Aerospace Conference*. 1–8. IEEE.

[4] Shapiro, A. A., *et al.* 2016. Additive Manufacturing for Aerospace Flight Applications. *Journal of Spacecraft and Rockets*. 53(5): 952–959.

[5] Khorasani, M., A. Ghasemi, B. Rolfe, and I. Gibson. 2022. Additive Manufacturing: A Powerful Tool for the Aerospace Industry. *Rapid Prototyping Journal*. 28(1): 87–100.

[6] Rodríguez-Salvador, M., and L. A. Garcia-Garcia. 2018. Additive Manufacturing in Healthcare. *Foresight and STI Governance*. 12(1): 47–55.

[7] Ghomi, E. R., F. Khosravi, R. E. Neisiany, S. Singh, and S. Ramakrishna. 2021. Future of Additive Manufacturing in Healthcare. *Current Opinion in Biomedical Engineering*. 17: 100255.

[8] Sun, L. 2022. 3D Printing and Additive Manufacturing in Fashion. In *Leading Edge Technologies in Fashion Innovation: Product Design and Development Process from Materials to the End Products to Consumers*. 59–74. Springer.

[9] Yap, Y. L., and W. Y. Yeong. 2014. Additive Manufacture of Fashion and Jewellery Products: A Mini Review. *Virtual and Physical Prototyping*. 9(3): 195–201.

[10] Liu, W., Z. Zhu, and S. Ye. 2019. Industrial Case Studies of Design for Plastic Additive Manufacturing for End-Use Consumer Products. *3D Printing and Additive Manufacturing*. 6(6): 281–292.

[11] Yoo, B., H. Ko, and S. Chun. 2016. Prosumption Perspectives on Additive Manufacturing: Reconfiguration of Consumer Products with 3D Printing. *Rapid Prototyping Journal*. 22(4): 691–705.

[12] Global Market Estimates. 2024. Fused Deposition Modeling (FDM) 3D Printing Market Analysis: Size. Accessed February 1, 2024. https://www.globalmarketestimates.com/market-report/fused-deposition-modeling-fdm-3d-printing-market-3944.

[13] Wickramasinghe, S., T. Do, and P. Tran. 2020. FDM-Based 3D Printing of Polymer and Associated Composite: A Review on Mechanical Properties, Defects and Treatments. *Polymers.* 12(7): 1529.
[14] Sandanamsamy, L., *et al.* 2023. A Comprehensive Review on Fused Deposition Modelling of Polylactic Acid. *Progress in Additive Manufacturing.* 8(5): 775–799.
[15] Baran, E. H., and H. Y. Erbil. 2019. Surface Modification of 3D Printed PLA Objects by Fused Deposition Modeling: A Review. *Colloids and Interfaces.* 3(2): 43.
[16] Cuiffo, M. A., J. Snyder, A. M. Elliott, N. Romero, S. Kannan, and G. P. Halada. 2017. Impact of the Fused Deposition (FDM) Printing Process on Polylactic Acid (PLA) Chemistry and Structure. *Applied Sciences.* 7(6): 579.
[17] Kamaal, M., M. Anas, H. Rastogi, N. Bhardwaj, and A. Rahaman. 2021. Effect of FDM Process Parameters on Mechanical Properties of 3D-Printed Carbon Fibre–PLA Composite. *Progress in Additive Manufacturing.* 6: 63–69.
[18] Chaudhry, F. N., S. I. Butt, A. Mubashar, A. Bin Naveed, S. H. Imran, and Z. Faping. 2022. Effect of Carbon Fibre on Reinforcement of Thermoplastics Using FDM and RSM. *Journal of Thermoplastic Composite Materials.* 35(3): 352–374.
[19] Heidari-Rarani, M., M. Rafiee-Afarani, and A. M. Zahedi. 2019. Mechanical Characterization of FDM 3D Printing of Continuous Carbon Fiber Reinforced PLA Composites. *Composites Part B: Engineering.* 175: 107147.
[20] Kim, H., and S. Lee. 2020. Characterization of Electrical Heating of Graphene/PLA Honeycomb Structure Composite Manufactured by CFDM 3D Printer. *Fashion and Textiles.* 7(1): 8.
[21] Camargo, J. C., Á. R. Machado, E. C. Almeida, and E. F. M. S. Silva. 2019. Mechanical Properties of PLA-Graphene Filament for FDM 3D Printing. *The International Journal of Advanced Manufacturing Technology.* 103: 2423–2443.
[22] Vidakis, N., M. Petousis, K. Savvakis, A. Maniadi, and E. Koudoumas. 2019. A Comprehensive Investigation of the Mechanical Behavior and the Dielectrics of Pure Polylactic Acid (PLA) and PLA with Graphene (GnP) in Fused Deposition Modeling (FDM). *International Journal of Plastics Technology.* 23(2): 195–206.
[23] Nofar, M., D. Sacligil, P. J. Carreau, M. R. Kamal, and M.-C. Heuzey. 2019. Poly (Lactic Acid) Blends: Processing, Properties and Applications. *International Journal of Biological Macromolecules.* 125: 307–360.
[24] Dicker, M. P. M., P. F. Duckworth, A. B. Baker, G. Francois, M. K. Hazzard, and P. M. Weaver. 2014. Green Composites: A Review of Material Attributes and Complementary Applications. *Composites Part A: Applied Science and Manufacturing.* 56: 280–289.
[25] Sun, Z., L. Zhang, D. Liang, W. Xiao, and J. Lin. 2017. Mechanical and Thermal Properties of PLA Biocomposites Reinforced by Coir Fibers. *International Journal of Polymer Science.* 2017(1): 2178329.
[26] Adeniyi, A. G., D. V. Onifade, J. O. Ighalo, and A. S. Adeoye. 2019. A Review of Coir Fiber Reinforced Polymer Composites. *Composites Part B: Engineering.* 176: 107305.
[27] Deka, H., T. O. Varghese, and S. K. Nayak. 2016. Recent Development and Future Trends in Coir Fiber-Reinforced Green Polymer Composites: Review and Evaluation. *Polymer Composites.* 37(11): 3294–3309.
[28] Chotiprayon, P., B. Chaisawad, and R. Yoksan. 2020. Thermoplastic Cassava Starch/Poly (Lactic Acid) Blend Reinforced with Coir Fibres. *International Journal of Biological Macromolecules.* 156: 960–968.
[29] Maglalang, P. E. C., B. A. Basilia, and A. M. Monsada. 2021. Investigating the Mechanical Behavior of 3D Printed PLA-Coco Coir Composites. In *Materials Science Forum*. 125–132. Trans Tech Publications.
[30] Ansaripour, A., and M. Heidari-Rarani. 2024. Hybrid Toughening Effect of Flax Fiber and Thermoplastic Polyurethane Elastomer in 3D-Printed Polylactic Acid Composites. *Polymer Composites.* 45(18): 17239–17256.
[31] Avci, A., A. A. Eker, and M. S. Bodur. 2021. Effect of Coupling Agent and Alkali Treatment on Mechanical, Thermal and Morphological Properties of Flax-Fiber-Reinforced PLA Composites. *Green Materials.* 9: 131–144.
[32] Heidari-Rarani, M., and F. Khajavirad. 2024. Challenges in Making Filaments for Fused Filament Fabrication 3D Printers. In *Additive Manufacturing Materials and Technology*, 127–171. Elsevier.
[33] Girish, B. M., H. S. Siddesh, and B. M. Satish. 2019. Taguchi Grey Relational Analysis for Parametric Optimization of Severe Plastic Deformation Process. *SN Applied Sciences.* 1(8): 937.
[34] Abeykoon, C. 2014. A Novel Model-Based Controller for Polymer Extrusion. *IEEE Transactions on Fuzzy Systems.* 22(6): 1413–1430.
[35] Abeykoon, C., P. J. Martin, A. L. Kelly, K. Li, E. C. Brown, and P. D. Coates. 2014. Investigation of the Temperature Homogeneity of Die Melt Flows in Polymer Extrusion. *Polymer Engineering and Science.* 54(10): 2430–2440.
[36] Tan, Y. A., M. Y. Chan, S. C. Koay, and T. K. Ong. 2023. 3D Polymer Composite Filament Development from Post-Consumer Polypropylene and Disposable Chopstick Fillers. *Journal of Vinyl and Additive Technology.* 29(5): 909–922.
[37] Hanim, N., M. D. Syafiq, Z. A. Abdul Hamid, A. Rusli, M. K. Abdullah, and R. K. Shuib. 2022. Fused Deposition Modelling of Flexible Kenaf Fiber/Thermoplastic Polyurethane Composites. *Progress in Rubber, Plastics and Recycling Technology.* 38(4): 328–342.
[38] Zhuang, Y., B. Zou, S. Ding, X. Wang, J. Liu, and L. Li. 2023. Preparation of Pre-Impregnated Continuous Carbon Fiber Reinforced Nylon6 Filaments and the Mechanical Properties of 3D Printed Composites. *Materials Today Communications.* 35: 106163.
[39] Sun, Q., G. M. Rizvi, C. T. Bellehumeur, and P. Gu. 2008. Effect of Processing Conditions on the Bonding Quality of FDM Polymer Filaments. *Rapid Prototyping Journal.* 14(2): 72–80.
[40] Chacón, J. M., M. A. Caminero, E. García-Plaza, and P. J. Núnez. 2017. Additive Manufacturing of PLA Structures Using Fused Deposition Modelling: Effect of Process Parameters on Mechanical Properties and Their Optimal Selection. *Materials and Design.* 124: 143–157.
[41] Lee, H.-N., K. Paeng, S. F. Swallen, and M. D. Ediger. 2009. Direct Measurement of Molecular Mobility in Actively Deformed Polymer Glasses. *Science.* 323(5911): 231–234.
[42] Rapp, P. B., A. K. Omar, B. R. Silverman, Z.-G. Wang, and D. A. Tirrell. 2018. Mechanisms of Diffusion in Associative Polymer Networks: Evidence for Chain Hopping. *Journal of the American Chemical Society.* 140(43): 14185–14194.
[43] Coogan, T. J., and D. O. Kazmer. 2017. Bond and Part Strength in Fused Deposition Modeling. *Rapid Prototyping Journal.* 23(2): 414–422.
[44] Ziemian, C., M. Sharma, and S. Ziemian. 2012. Anisotropic Mechanical Properties of ABS Parts Fabricated by Fused Deposition Modelling. *Mechanical Engineering.* 23: 159–180.
[45] Wang, C., J. Li, and C. Zhang. 2025. Effect of Corrected Extrusion Flow Rate on Wall Thickness Error of MEAM Thin-Walled Model. *Materiale Plastice.* 62(1).
[46] Schöppner, V., and M. Pohl. 2019. High Speed Extrusion of Modified Polycarbonate. In *AIP Conference Proceedings*. AIP Publishing.
[47] Kechagias, J. D., N. A. Fountas, I. Papantoniou, and N. M. Vaxevanidis. 2025. Interlaminar Bonding Assessment in Vertical-Oriented Filament Material Extrusion Bending Specimens. *The International Journal of Advanced Manufacturing Technology.* 1–13.
[48] Klosterman, D., C. Browning, I. Hakim, and K. Lach. 2021. Investigation of Various Techniques for Controlled Void Formation in Fiberglass/Epoxy Composites. *Journal of Composite Materials.* 55(4): 489–506.
[49] Bergaliyeva, S., *et al.* 2023. Thermal and Mechanical Properties of Reprocessed Polylactide/Titanium Dioxide

Nanocomposites for Material Extrusion Additive Manufacturing. *Polymers.* 15(16): 3458.
[50] Lunt, B. M., C. Buntel, and M. R. Linford. 2009. Embrittlement of Polycarbonate Optical Discs. *Journal of Advanced Materials.* 41(4): 22–27.
[51] Lee, S., and J.-W. Wee. 2024. Effect of Temperature and Relative Humidity on Hydrolytic Degradation of Additively Manufactured PLA: Characterization and Artificial Neural Network Modeling. *Polymer Degradation and Stability.* 230: 111055.
[52] Kausch, H. H. 2005. The Effect of Degradation and Stabilization on the Mechanical Properties of Polymers Using Polypropylene Blends as the Main Example. In *Macromolecular Symposia*. 165–178. Wiley Online Library.